



Citation for published version:

Koulountzios, P, Rymarczyk, T & Soleimani, M 2021, 'Handwriting with sound-speed imaging using ultrasound computed tomography.', *IEEE Sensors Letters*, vol. 5, no. 10, 5501003.
<https://doi.org/10.1109/LENS.2021.3109152>

DOI:

[10.1109/LENS.2021.3109152](https://doi.org/10.1109/LENS.2021.3109152)

Publication date:

2021

Document Version

Peer reviewed version

[Link to publication](#)

© 2021 IEEE. Personal use of this material is permitted. Permission from IEEE must be obtained for all other users, including reprinting/ republishing this material for advertising or promotional purposes, creating new collective works for resale or redistribution to servers or lists, or reuse of any copyrighted components of this work in other works.

University of Bath

Alternative formats

If you require this document in an alternative format, please contact:
openaccess@bath.ac.uk

General rights

Copyright and moral rights for the publications made accessible in the public portal are retained by the authors and/or other copyright owners and it is a condition of accessing publications that users recognise and abide by the legal requirements associated with these rights.

Take down policy

If you believe that this document breaches copyright please contact us providing details, and we will remove access to the work immediately and investigate your claim.

Handwriting with sound-speed imaging using ultrasound computed tomography.

P Koulountzios¹, T Rymarczyk², M Soleimani^{1*}

¹ Engineering Tomography Laboratory (ETL), Department of Electrical and Electronic Engineering, *University of Bath, UK*

² Research & Development Centre Netrix S.A., Wojciechowska 31, 20-704 Lublin, Poland

Abstract— This work proposes the use of ultrasound computed tomography (USCT) for handwriting by imaging sound velocity changes in a medium caused by a rod. The rod was used as a writing object and the tomographic instrument was able to process the data over time with a temporal frequency of 4 frames per second. Tests are carried out in writing various words and letters using USCT data and automatic imaging software. The work shows the functional imaging capability offered by the USCT system combining qualitative and temporal imaging features.

Index Terms—In-water handwriting, electrical impedance tomography, dynamical inverse problems

I. INTRODUCTION

Human-computer interaction (HCI) techniques have been extensively developed in the past few years [1], [2], [3]. There is great interest in motion and gesture detection [6], [7], [8]. Earlier on [4], [5] the possibility of handwriting in water, by disturbing the pattern of electrical current, was demonstrated using electrical impedance tomography. The paper shows a new type of HCI using ultrasound computed tomography (USCT) with an experimental demonstration in producing handwriting of letters and words. The USCT has been lately developed for breast cancer imaging with clinical success [9], [10], and in industrial process monitoring [11], [12], [13], [14]. The common scientific topic that USCT can take advantage of in all these applications is high-quality imaging over time combining qualitative and temporal features with significant outcomes. USCT, in that sense, could aid other tools that have been researched already in the handwriting field. The study shows that USCT can act as a communication tool in HCI applications by showing its feasibility for handwriting.

II. USCT SYSTEM

USCT includes a hardware system for data acquisition, an array of ultrasound sensors and software to support data collection and image reconstruction. The developed ultrasound tomography is based on a parallel data transferring architecture. Its main attribute is the active measurement probes. The probes are controlled by a CAN bus, which works as an external module, avoiding the use of a host computer. Therefore, the process turns to be less time-consuming transferring and receiving data much faster. This design can exclude a switching part from the system, while the receivers should be in the “receiving mode”. Subsequently, a multiplexer, which would introduce

additional delays, is neglected. Active measuring probes are divided into digital and analogue parts. The digital part is responsible for sending measurement data to the tomography controller, via the bus. The analogue part has been adapted to work with the piezoelectric transducer. The active probe can work both as a receiver and as a transmitter. The main controller is responsible for managing the measurement sequence, setting the active probes in the transmit/receive mode, as well as storing the recorded information [15]. In this study, the sensors are mounted outside of a water-filled tank with a central excitation frequency of 40 kHz. USCT has several modes of operations such as travel-time imaging, reflection mode imaging and amplitude attenuation imaging. In fact, each one of these modes could be used for such an HCI application proposed here. In this study, we use the travel-time imaging [16] with 16 sensor arrays surrounding a tank as shown in figure 1. A plastic rod is used for its varying speed of sound against the background water to alter the sound velocity distribution inside the tank water. The USCT system can produce 4 frames of USCT images per each sec, proving a high temporal resolution and allowing smooth handwriting.

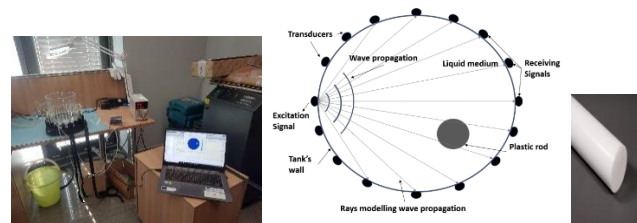


Fig. 1: (a) USCT measurement system on an acrylic tank of 20cm. (b) USCT's functionality. (c) Plastic rod, used as an inclusion in the experimental process.

This work was supported by the European Union's Horizon 2020 research and innovation programme under the Marie Skłodowska-Curie Grant 764902.

M Soleimani and P Koulountzios are with Engineering Tomography Lab (ETL), University of Bath, UK. T Rymarczyk with Research & Development Centre Netrix S.A., Wojciechowska 31, 20-704 Lublin, Poland;

Corresponding author: M.S. Author (m.soleimani@bath.ac.uk). Digital Object Identifier: 10.1109/LSN.XXXX.XXXXXXX (inserted by IEEE).

A. Forward problem

For the travel-time transmission tomography method, a ray-based method was used. The ray trajectories are calculated by solving equation (1) and accounting for very high emission frequencies [17].

$$\frac{d}{ds} \left(\frac{1}{c} \frac{dx}{ds} \right) = \frac{1}{c^2} \nabla c \quad (1)$$

where s is the length of the ray in the path of the sound wave, x is the physical position and c is the speed of sound. The ray-approximation approach can be used to simplify the relationship between sound speed on the path of ray and total travel time between transmission and receiving sensors:

$$\Delta m = \int_{ray} \Delta v(x) dl \quad (2)$$

The above integral is based on a single ray path, Δv denotes the sound velocity domain and Δm gives the time of flight of the pulse. For a generalized tomographic problem, the above equation (2) can be expressed as:

$$\Delta m = J \Delta v + e \quad (3)$$

Where Δm is the time-of-flight perturbation, J is the modelling operator which expresses the sensitivity distribution and Δv is the sound speed and e is the noise in measured time of flight.

B. Inverse problem

A simple inversion algorithm could involve using a linear back projection (LBP):

$$\Delta v = J' \Delta m \quad (4)$$

The LBP is a simple algorithm and produces images together with an extensive amount of image artefact. Instead, we are using a dynamical Tikhonov regularization algorithm [7]. This method allows multiple frames of data $\widetilde{\Delta m}_t = [\Delta m_{t-d}; \dots; \Delta m_t; \dots; \Delta m_{t+d}]$ to be reconstructed simultaneously and allowing to reconstruct the sound speed in time steps $\widetilde{\Delta v}_t = [\Delta v_{t-d}; \dots; \Delta v_t; \dots; \Delta v_{t+d}]$. Therefore, the temporal inverse problem can be rewritten as

$$\widetilde{\Delta v}_t = S \widetilde{\Delta m}_t \quad (5)$$

where S is a precalculated dynamical Tikhonov inverse matrix. This will have the same computational time as simple LBP but provide both spatial and temporal regularization. Image normalization is then conducted in the same way as [4].

III. EXPERIMENTS AND RESULTS

The image reconstruction is done with the differential data where measured data with the plastic rod is compared with the background data. Figure 2 shows the time of flight measurement data for 240 independent measurements from 16 sensor arrays. It is possible to measure 256 travel time data, but we exclude the receiving time data for transmitting sensors leading to 240 measurements.

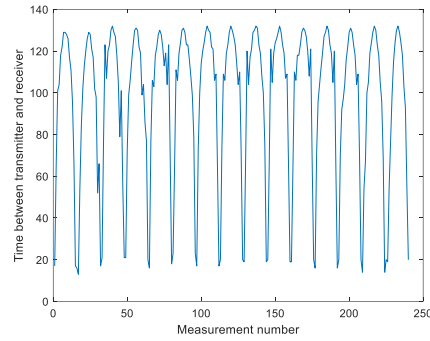


Fig. 2: Measured background data.

A. Single Letter

The letters are produced by using multiple frames of USCT image each contributing to the path of the shape of the letter. Fig. 3(a) presents the consecutive reconstructed frames, the synthesized image of a letter “S” and the normalized values of the difference data. A total of 31 informative frames have been recorded for this case. Filter algorithm excludes frames that do not contain substantial information, resulting in 23 processed frames. Finally, 12 frames were presented for the total number of processed frames using step two. The displayed frames start from the 8th frame. Earlier frames have been excluded by the filter. Frames of data will act as a dot in the letter “S”. For all the 240 measured data, Root mean square difference (RMSD) which is the norm of differences between background and inclusion data, is used to space between letters.

B. Combined letters

This section presents cases of word recognition and word formation. Fig. 4 shows the letters of words “UST”, “DAN”, “HAN”, “manuch”, “netrix”, “Soleimani”, “tomography”. In most cases, the system was able to distinguish between different letters of the alphabet and offer the real genuine hand-writing style without losing the quality features of reconstructions.

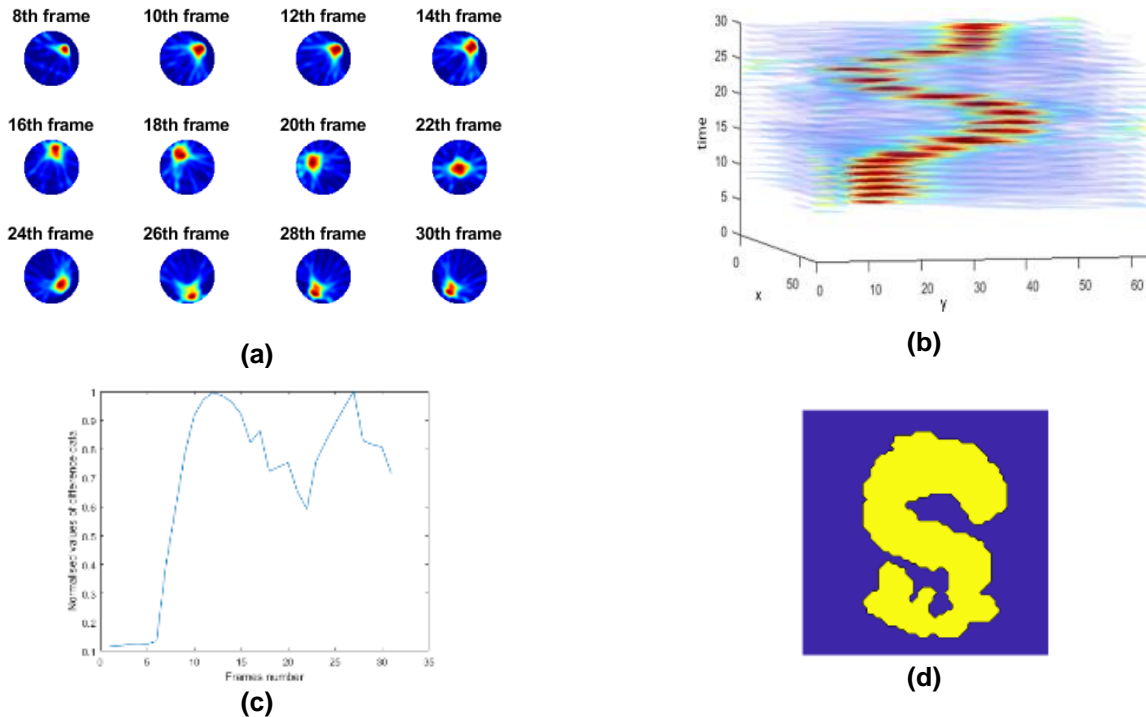
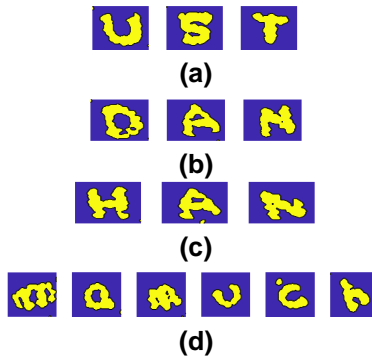


Fig 3: (a) Frames of USCT images used to construct letter “S”. (b) Plot of the reconstructed 3D volumetric dataset. (c) RMSD for all frames. (d) Reconstructed image of letter “S”.

The reconstruction of complex words and letters suggest that a simple USCT system such as the one used in here, although it may be with low spatial resolution can reveal satisfactory functional information.

For the test case of word ‘UST’, 94 frames of USCT images were considered, and the norm differences between background and inclusion for this word are shown in Fig. 5. Given the “between words” specific movement of slightly getting the rod outside of the field-of-view (FOV) (lifting of the rod), the norm difference data tend to decrease into a minimum level and subsequently can be used to create spaces between letters.

A small value of the norm difference suggests that the pen is out of sight of the sensor array, and this allow space between letters. Hence, one can see the distinct frame window of each letter in the word. Moreover, the number of close-to-zero regions in the function of norms over frames can indicate the number of word’s characters. Using machine learning one can enhance letter and word recognition, but this can be studied in future. Adapting such a low-cost system for real-time motion recognition can offer great potential to many applications, as ultrasounds can be used in the water, soil, air and almost all the common media of the environment.



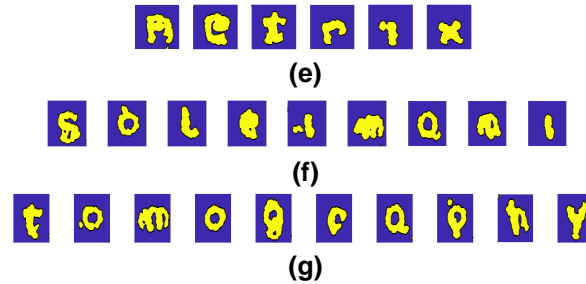


Fig. 4: Reconstruction of word (a) UST, (b) DAN, (c) HAN, (d) manuch, (e) netrix, (f) soleimani, (g) tomography

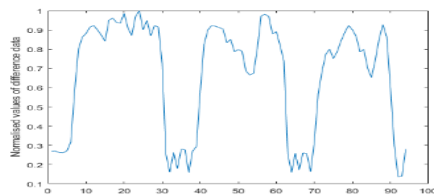


Fig. 5: RMSD in the "UST" word test.

IV. CONCLUSIONS

The paper shows the use of USCT for hand-writing and it was shown both to recognize letters and forming words. For this work, water as propagating medium and sensors of 40 kHz were used. It shows the versatility of USCT when imaging a functional act such as real time handwriting. The USCT system should have sufficient frame rate allowing a natural handwriting experience 4 frames per second used in this paper seems fast enough. The artefacts in individual point of images can be removed, but for drawing a more complex shape one needs to be able to use a smaller rod. In that case we need to ensure that the USCT system can detect the smaller rod in all areas of water tank. It is possible to extend the method for sound velocity imaging in air making it a suitable device for motion and gesture tracking, but in air handwriting the method needs to compete with well established HCI methods such as optical based system. The entire process shown here can show a flexible use of USCT to map out complex events demonstrating even with low spatial resolution, the high temporal resolution may lead to imaging complicated dynamical situation.

REFERENCES

- [1] A. Erol, G. Bebis, M. Nicolescu, R. D. Boyle, and X. Twombly, "Vision-based hand pose estimation: a review," *Computer Vision and Image Understanding*, vol. 108, no. 1-2, pp. 52–73, 2007.
- [2] S. Mitra and T. Acharya, "Gesture recognition: a survey," *IEEE Transactions on Systems, Man and Cybernetics Part C: Applications and Reviews*, vol. 37, no. 3, pp. 311–324, 2007.
- [3] S. Berman and H. Stern, "Sensors for gesture recognition systems," *IEEE Transactions on Systems, Man and Cybernetics, Part C: Applications and Reviews*, vol. 42, no. 3, pp. 277–290, 2012.
- [4] C. Wu and M. Soleimani, "In-water handwriting in multi-medium using electrical impedance imaging," *IOPSciNotes* 1 025001, 2020.
- [5] T. Zhao, C. Wu, M. Soleimani, "Ionic liquid based distributed touch sensor using electrical impedance tomography." *IOPSciNotes* 1 025005, 2020.
- [6] C. Amma, M. Georgi, T. Schultz, "Airwriting: Hands-free mobile text input by spotting and continuous recognition of 3d-space handwriting with inertial sensors." In: *International symposium on wearable computers*, pp 52–59, 2012.
- [7] M. Chen, G. Alregib, B.H. Juang, "Air-writing recognition-part i: modeling and recognition of characters, words, and connecting motions" *IEEE Trans. Hum.-Mach. Syst.*, 46 (3) (2016), pp. 403-413.
- [8] J. Gan and W. Wang, "In-air handwritten English word recognition using attention recurrent translator," *Neural Computing and Applications* volume 31, pages3155–3172(2019).
- [9] F. M. Hooi and P. L. Carson, "First-arrival traveltime sound speed inversion with a priori information," *Med. Phys.*, vol. 41, no. 8, pp. 1–14, 2014.
- [10] I. Peterlik, R. Jiřik, N. Ruiter, and J. Jan, "Regularized image reconstruction for ultrasound attenuation transmission tomography," *Radioengineering*, vol. 17, no. 2, pp. 125–132, 2008.
- [11] H. I. Schlaberg, M. S. Beck, B. S. Hoyle, C. Lenn, and Ming Yang, "Real-time ultrasound process tomography for two-phase flow imaging using a reduced number of transducers," *IEEE Trans. Ultrason. Ferroelectr. Freq. Control*, vol. 46, no. 3, pp. 492–501, 2002.
- [12] N. Muzakkir, N. Ayob, M. Hafiz, F. Rahiman, S. Yaacob, and R. A. Rahim, "Ultrasound Processing Circuitry for Ultrasonic Tomography," 2009.
- [13] C. Tan, X. Li, H. Liu, and F. Dong, "An ultrasonic transmission/reflection tomography system for industrial multiphase flow imaging," *IEEE Trans. Ind. Electron.*, vol. 66, no. 12, pp. 9539–9548, Dec. 2019.
- [14] H. Liu, C. Tan, and F. Dong, "Continuous-wave ultrasonic tomography for oil/water two-phase flow imaging using regularized weighted least square framework," *Trans. Inst. Meas. Control*, vol. 42, no. 4, pp. 666–679, 2020.
- [15] R. Tomasz, G. Michal, B. Piotr, A. Przemyslaw, M. Michal and S. Jan, "The prototype ultrasound tomography device to analyze the properties of processes," *2018 Applications of Electromagnetics in Modern Techniques and Medicine (PTZE)*, 2018, pp. 228-231, doi: 10.1109/PTZE.2018.8503197.
- [16] P. Koulountzios, T. Rymarczyk, and M. Soleimani, "Ultrasonic Tomography for automated material inspection in liquid masses," 9th World Congr. Ind. Process Tomogr. WCIPT9, Sep 2018, pp. 693–702, 2018.
- [17] Kravtsov, Y.A.; Orlov, Y.I. *Geometrical Optics of Inhomogeneous Media*; Springer: New York, NY, USA, 1990.